



ELSEVIER

International Journal of Mass Spectrometry 182/183 (1999) 275–288



# Ion internal temperature and ion trap collisional activation: protonated leucine enkephalin

Douglas E. Goeringer, Keiji G. Asano, Scott A. McLuckey\*

*Chemical and Analytical Sciences Division, Oak Ridge National Laboratory, Oak Ridge, TN 37831-6365, USA*

Received 16 July 1998; accepted 16 September 1998

## Abstract

Protonated leucine enkephalin has been used as a prototypical high-mass ion to yield a quantitative estimate of the relationship between the amplitude of the resonance excitation voltage used in an ion trap collisional activation experiment, and the internal temperature to which an ion can be elevated over the bath gas temperature. The approach involves the measurement of the ion dissociation rate as a function of resonance excitation voltage, and the correlation of dissociation rate with ion internal temperature. The relatively high ion trap dissociation rates observed under typical resonance excitation conditions preclude the direct application of the Arrhenius equation to derive internal temperatures. An empirical determination of the relationship between ion internal temperature and dissociation rate over the rate range of interest here was made via the systematic variation of bath gas temperature. The data suggest a very nearly linear relationship between ion internal temperature and resonance excitation voltage, at least under conditions in which ion ejection is minimal. It is shown that protonated leucine enkephalin ions can be elevated by about 357 K over the bath gas temperature using a monopolar resonance excitation voltage of 540 mV  $p - p(q_z = 0.163)$  without significant ion ejection. It is also demonstrated that ion internal temperature can be readily increased by increasing the bath gas temperature, by accelerating the ions in the presence of a room temperature bath gas (i.e. conventional ion trap collisional activation), or by a combination of the two approaches. (Int J Mass Spectrom 182/183 (1999) 275–288) © 1999 Elsevier Science B.V.

*Keywords:* Quadrupole ion trap; Ion activation; Collisional activation; Ion internal temperature

## 1. Introduction

The appearance of a collision-induced dissociation (CID) spectrum is a function of fundamental properties of the ion, such as the energies and entropies of the various competitive decomposition channels, the time window of observation, and the internal energy distribution,  $P(\epsilon)$ , of the ion population [1–3]. To

draw reliable conclusions about fundamental properties of the ions, knowledge of or control over the time window of observation and  $P(\epsilon)$  is necessary. In most forms of tandem mass spectrometry, it is straightforward to determine the time window of observation. However,  $P(\epsilon)$  in collisional activation experiments is usually very difficult to determine. For this reason, the subject of internal energy distributions in tandem mass spectrometry over the wide variety of collisional activation conditions that have been employed has been the subject of much research [1–8].

Activation methods in tandem mass spectrometry

\* Corresponding author. E-mail: mcluckeya@oml.gov  
Dedicated to the memory of Professor Ben Freiser.

in general can be classified according to the time frame or rate of activation relative to the rates of fragmentation and deactivation [9]. An increasingly important subset of activation methods, typically conducted in tandem mass spectrometers capable of storing ions on the order of tens of milliseconds or longer, has been referred to as slow heating or very slow activation [9]. Prominent examples include multiphoton infrared dissociation [10–26], driven either by a continuous-wave infrared laser [10–16] or by blackbody radiation [17–26], and ion trap collisional activation [27,28]. These methods are characterized by the condition that activation, deactivation, and dissociation all occur in parallel with the rates of activation and deactivation being nearly equal. The ions reach a steady-state internal energy distribution which approximates a true Boltzmann distribution when the rates of activation and deactivation are much greater than unimolecular dissociation rates or a so-called truncated Boltzmann distribution [13] when unimolecular dissociation rates rival or are greater than the activation/deactivation rates. For the former condition, in particular, the parent ion  $P(\epsilon)$  can be characterized by a temperature.

In this article, we describe experiments with protonated leucine enkephalin designed to determine the  $P(\epsilon)$  expressed in terms of an internal temperature,  $T_{\text{int}}$ , achieved under typical single-frequency resonance excitation [27] conditions in a quadrupole ion trap. Random walk modeling of single-frequency resonance excitation, making a simple forced damped harmonic oscillator approximation for the ion acceleration process, has shown that in the absence of fragmentation, parent ions achieve a steady-state Boltzmann internal energy distribution during resonance excitation [29,30], as expected for a slow heating method. The values of the internal temperatures yielded by modeling are, in part, a function of assumptions made in modeling ion acceleration and rates of energy transfer. Experimental measurements, such as those described herein, facilitate refinement of the parameters used in the modeling and give empirical data obtained from resonance excitation in an ion trap with higher order fields intentionally imposed [31,32]. Measurements of the type reported here will

be required for a wide variety of parent ions, including both diatomic ions and high mass polyatomic ions, before a comprehensive picture of the relationship between resonance excitation conditions and parent ion internal energies can be drawn. This article constitutes the first report of a quantitative measurement of parent ion internal temperatures achieved under ion trap resonance excitation conditions for any type of ion. This work has focused on a relatively high-mass ion because at constant dissociation rates the characterization of  $P(\epsilon)$  with a temperature is increasingly accurate as the size of the ion increases [26]. That is, for a fixed observed dissociation rate, the degree to which the parent ion internal energy distribution deviates from a true Boltzmann distribution decreases as ion size increases.

This work augments literature data on ion trap collisional activation of relatively small organic ions in which *average* internal energies were reported based on the appearance of product ion spectra of “thermometer” ions [27,28,33–36], such as ionized *n*-butylbenzene. It is important to recognize that the use of relative product ion abundances as a gauge of parent ion internal energy selects only for parent ions that fragment. As such, the product ion spectrum does not directly reflect the internal energies of the activated ions that do not fragment within the time frame of the experiment. Furthermore, the use of ion abundances as a measure of parent ion internal energy requires the assumption that energy input or removal from first generation products ions does not occur to a significant extent. This assumption becomes increasingly questionable as the size of the parent ion increases [37]. It has been demonstrated that information about ion energetics can also be derived using ion trap collisional activation from the rates of parent ion dissociation [38,39]. Provided information is already known about the energy and entropy requirements for dissociation, ion dissociation rates can be used to draw conclusions regarding the parent ion internal energy distribution, as has recently been demonstrated for dissociation of protonated leucine enkephalin induced by heating the bath gas in the ion trap [40]. Therefore, parent ion dissociation rates under collisional activation conditions are used in this work,

along with master equation modeling, to draw conclusions about ion internal temperatures achievable under normal ion trap collisional activation conditions for a protonated peptide. Leucine enkephalin was chosen as the model system because its dissociation kinetics have already been studied by heated bath gas experiments in a quadrupole ion trap [40], blackbody infrared radiative dissociation [41], and heated capillary dissociation in an electrospray ionization source [42].

## 2. Experimental section

Leucine enkephalin (tyr-gly-gly-phe-leu or YG-GFL) obtained commercially (Sigma, St. Louis, MO) was dissolved in a solution of 50:50 methanol:water to a concentration of roughly 2160  $\mu\text{M}$  with 1% acetic acid. Working solutions ( $\sim 30 \mu\text{M}$ ) were prepared by diluting the stock solution with 99% methanol/1% acetic acid. The solution was infused at a rate of 1.0  $\mu\text{L}/\text{min}$  through a 100  $\mu\text{m}$  inner diameter (i.d.) stainless steel capillary held at +3.5–4.0 kV.

All experiments were performed with a Finnigan Ion Trap Mass Spectrometer (ITMS, Finnigan Corp., San Jose, CA), modified for electrospray ionization. An electrospray interface/ion injection lens/ion trap assembly, which has been described previously [43], was attached to the vacuum system of the ITMS. The ITMS vacuum system is equipped with infrared heaters and a closed-loop temperature control system. A constant bath gas temperature was achieved by suspending the platinum resistance thermometer of the temperature control system in the vacuum system (i.e. it was disconnected from its normal attachment to the surface of the vacuum system). The temperature indicated by the platinum resistance thermometer was calibrated against a temperature measurement made by suspending a temperature probe (Omega) adjacent to the ion trap (in the absence of any applied voltage) and systematically altering the temperature set point of the temperature feedback system. Essentially identical temperatures were also measured when the probe was physically touching a mounting bracket of the ion trap electrodes. In all cases, helium was introduced

into the vacuum chamber to a total pressure (uncorrected) of  $1.1 \times 10^{-4}$  Torr, as measured on the ion gauge.

Following an ion accumulation period of 100–300 ms, protonated leucine enkephalin ions were isolated using a single resonance ejection ramp. That is, isolation of the parent ion of interest was effected using a single scan of the rf-voltage amplitude applied to the ring electrode while simultaneously applying a single frequency in monopolar fashion chosen to sweep out ions of mass-to-charge ratio greater than that of the ion of interest. Lower mass-to-charge ratio ions were swept out by passing the ions through the  $q_z = 0.908$  exclusion limit. A relatively broad ion isolation window (i.e. several mass-to-charge ratio units) was employed to avoid collisional activation of the parent ion by off-resonance power absorption because of the isolation step.

The rates of dissociation of the parent ions were measured by recording the product ion mass spectra as a function of activation time, as defined by the resonance excitation period, and as a function of either bath gas temperature or resonance excitation voltage amplitude, reported in terms of millivolts peak-to-peak. In the former case, resonance excitation voltage was held constant while the bath gas temperature was varied and in the latter case the bath gas temperature was held constant as the resonance excitation voltage was varied. In all cases, the parent ion was held at a  $q_z$  value of 0.163. The spectrum used for each reaction time was the average of 100 repetitions of the experimental sequence described above.

All studies were conducted under conditions in which changes in ion losses were minimal over the range of bath gas temperatures and resonance excitation conditions employed. Plots of total ion signal after the activation period divided by total ion signal before activation averaged between 0.8–0.9 over the entire temperature and resonance excitation voltage ranges studied. For this reason, resonance ejection is not expected to play a significant role in these studies. The complete data set described here was collected with one of the end-cap electrodes (inadvertently) grounded. Therefore, the resonance excitation voltages reported here apply to a situation in which

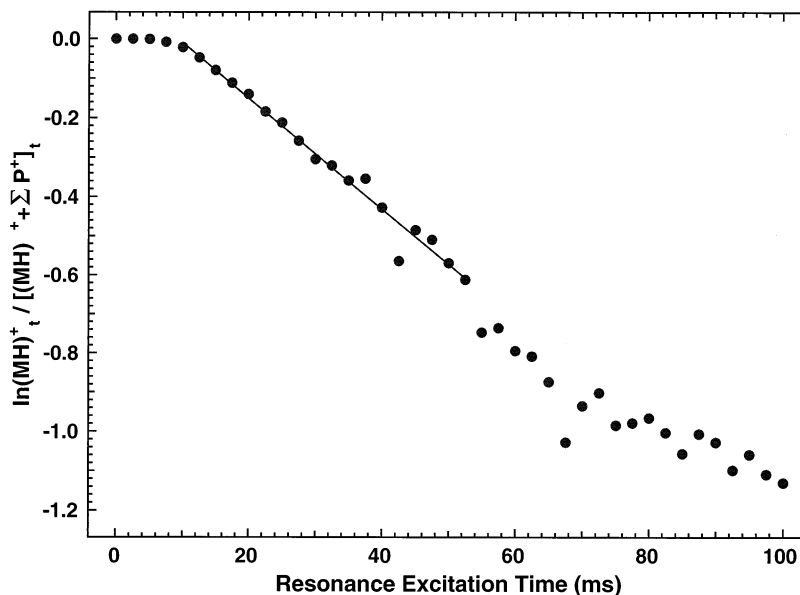


Fig. 1. A plot of  $\ln [MH^+]_t / [MH^+ + \Sigma P^+]_t$  vs. time using a monopolar resonance excitation amplitude of 400 mV ( $q_z = 0.163$ ) and room temperature helium (298 K), where  $MH^+$  is the protonated leucine enkephalin signal and  $\Sigma P^+$  is the sum of the signals of the product ions.

monopolar excitation was effected [44]. Similar results are expected using dipolar excitation, wherein equal frequencies and voltages are applied to the end caps, but of opposite phase, at resonance excitation voltage amplitudes of one half those reported here.

### 3. Results and discussion

The dissociation kinetics of an isomerically pure parent ion population in thermal equilibrium with its environment show a linear dependence of the natural logarithm of parent ion abundance versus time. The negative of the slope of such a plot gives the dissociation rate, and the intercept at time zero is  $\ln 1 = 0$ . This situation prevails, for example, with blackbody infrared radiative dissociation [17–26,41] and with dissociation driven in an ion trap by a heated bath gas [40]. Ions subjected to single-frequency resonance excitation are not in thermal equilibrium with the bath gas. The accelerated ion population, in the absence of fragmentation, assumes a Boltzmann distribution of internal energies characterized by a temperature somewhat greater than that of the bath gas [9]. The

steady-state parent ion internal energy distribution that is achieved once there is a steady-state velocity distribution, be it either Boltzmann or a truncated Boltzmann distribution, gives rise to the expected  $\ln$  (parent ion number) versus time relationship; but the (induction) time required to achieve this steady-state distribution gives rise to a nonzero intercept. Fig. 1 shows a plot of  $\ln [MH^+]_t / [MH^+ + \Sigma P^+]_t$  versus time using a resonance excitation amplitude of 400 mV and room temperature helium, where  $MH^+$  is the signal from protonated leucine enkephalin and  $\Sigma P^+$  is the sum of the product ion signals. Note that very little parent ion dissociation occurs during the first 10 ms of resonance excitation. After this brief induction period, the expected linear decrease in parent ion abundance is observed over a range of many tens of milliseconds. Finally, at long times it is unclear whether linear kinetics continue to prevail. This may simply be a reflection of poor ion statistics or some other phenomenon, such as a shift in parent ion frequency with ion number, that results in the residual parent ions falling out of resonance with the excitation signal. In any case, the intermediate time window (10–50 ms in the

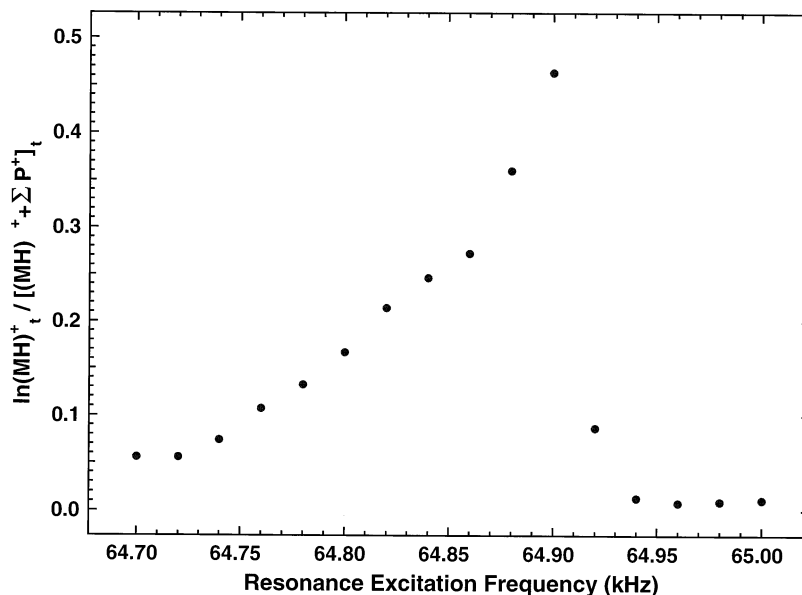


Fig. 2. A plot of  $\ln [\text{MH}^+]_t / [\text{MH}^+ + \sum \text{P}^+]_t$ , where  $t = 45$  ms, vs. resonance excitation frequency using a monopolar resonance excitation amplitude of 400 mV.

case of Fig. 1) can be used to measure a dissociation rate,  $k_{\text{diss}}$ , under ion trap collisional activation conditions. The dissociation rate can, in turn, be related to parent ion internal temperature (see below). The induction period necessary before linear dissociation kinetics is observed includes the rise time for the full resonance excitation amplitude specified by the software, the time required for the parent ion population to achieve a steady-state velocity distribution, and the time required for the parent ion population to achieve a steady-state internal energy distribution [38,45–47]. Linear dissociation kinetics do not prevail until the parent ion internal energy distribution completes its transition from the initial to final steady-state condition. The data points collected during the induction period are therefore not used to determine approximate parent ion temperatures at steady state.

A number of experimental variables are expected to play roles in determining the  $P(\epsilon)$  of parent ions under single frequency resonance excitation conditions in commonly used ion trap geometries that are often designed to include contributions from higher order fields [31,32]. In this work, we are primarily focused on the role of resonance excitation voltage

amplitude ( $V$ ) with all other variables held constant. This condition can be difficult to maintain as a result of interdependencies of some of the variables. Of particular importance for this work is the interdependence between  $V$  and optimum resonance frequency, defined here as that frequency which gives the highest dissociation rate for a given amplitude [38]. This frequency shifts with ion oscillatory amplitude as a result of the presence of higher order fields [32,38,48–51]. As a direct consequence of the increasing ion oscillatory amplitude resulting from increasing  $V$ , the resonance excitation frequency must be tuned at each voltage amplitude to ensure that the maximum ion dissociation rate is attained. Fig. 2 shows a plot of  $\ln [\text{MH}^+]_t / [\text{MH}^+ + \sum \text{P}^+]_t$ , where  $t = 45$  ms, as a function of resonance excitation frequency using a resonance excitation voltage of 400 mV. As expected, this plot shows the commonly observed shape associated with the absorption of power as a function of resonance excitation frequency in a so-called “stretched” ion trap [48–51,38] wherein the end-cap electrodes are spaced at a distance somewhat greater than the theoretical  $\sqrt{2}r_o$  distance, where  $r_o$  is the ring-electrode radius, for a pure

quadrupole field. For this excitation voltage, this plot reflects the frequency range over which sufficient ion heating occurs to drive dissociation rates to levels normally required in typical ion trap experiments (i.e. 1–500 s<sup>-1</sup>). The optimum frequency shifts to higher values as  $V$  increases because, as ion oscillatory amplitude increases, the higher order fields present in a stretched ion trap increase their influence on ion motion [32,38,48–51]. Furthermore, the frequency range over which readily measured dissociation rates are observed increases with  $V$ , as expected from the larger power absorption bandwidth associated with larger excitation voltages. A frequency tuning procedure was used prior to each kinetics experiment involving a fixed resonance excitation voltage. Tuning was performed by setting the resonance excitation or “tickle” time to a value that gave a roughly 50% diminution of the parent ion signal at a roughly optimized resonance excitation frequency and stepping the frequency by 20 Hz increments to minimize the parent ion signal. The frequency that minimized the parent ion signal was then used to collect data as a function of tickle time to determine the dissociation rate.

Fig. 3(a) shows a summary of the  $\ln [MH^+]/[MH^+ + \Sigma P^+]_t$  versus time data collected for a series of resonance excitation voltages. Fig. 3(b) shows a plot of the dissociation rates obtained from the slopes of the data in Fig. 3(a) over time periods in which linear kinetics were observed (i.e. after the induction period). The data points represent the frequency optimized rates at each resonance excitation voltage, as discussed in the preceding paragraph. The data clearly show, as expected, that the dissociation rate increases with resonance excitation voltage. Moreover, the increase in  $k_{\text{diss}}$  with  $V$  over the rate range reflected in Fig. 3(a) is clearly greater than linear [30].

Whereas it is clear that  $k_{\text{diss}}$  should increase with parent ion internal energy and that parent ion internal energy should be a function of  $V$ , it is not clear if the shape of the  $k_{\text{diss}}$  versus  $V$  curve of Fig. 3(b) is effected by nonlinearity in the ion acceleration process. Fig. 4 shows a plot of  $k_{\text{diss}}$  acquired as a function of bath gas temperature using a resonance excitation voltage of 300 mV. This combination of resonance

excitation voltage and bath gas temperatures was selected to yield  $k_{\text{diss}}$  values over a range that overlaps that of Fig. 3(a). In this case, ion acceleration conditions were held constant and ion activation conditions were varied in a known fashion by increasing the bath gas temperature (i.e. by increasing the kinetic energy of the bath gas). In analogy with the  $k_{\text{diss}}$  versus  $V$  behavior of Fig. 3(b),  $k_{\text{diss}}$  shows a greater than linear dependence upon bath gas temperature. This comparison indicates that the greater than linear increase in  $k_{\text{diss}}$  with  $V$  is not simply a result of a peculiarity of the ion acceleration process.

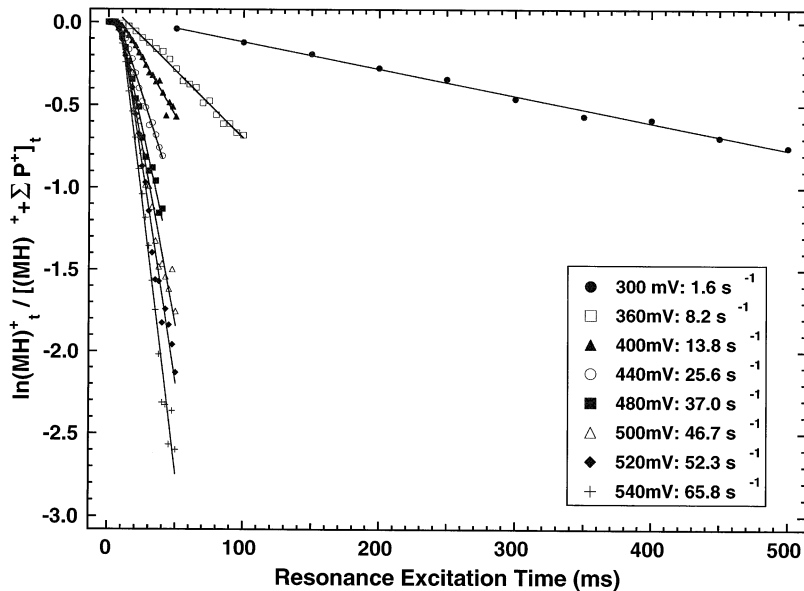
To draw conclusions about the parent ion internal energy dependence upon  $V$ , the quantitative relationship between  $k_{\text{diss}}$  and parent ion internal energy must be established. As a first approximation, use might be made of the Arrhenius rate equation that describes the relationship between  $k_{\text{diss}}$  and  $T_{\text{int}}$ , viz:

$$k_{\text{diss}} = Ae^{-E_a/kT_{\text{int}}} \quad (1)$$

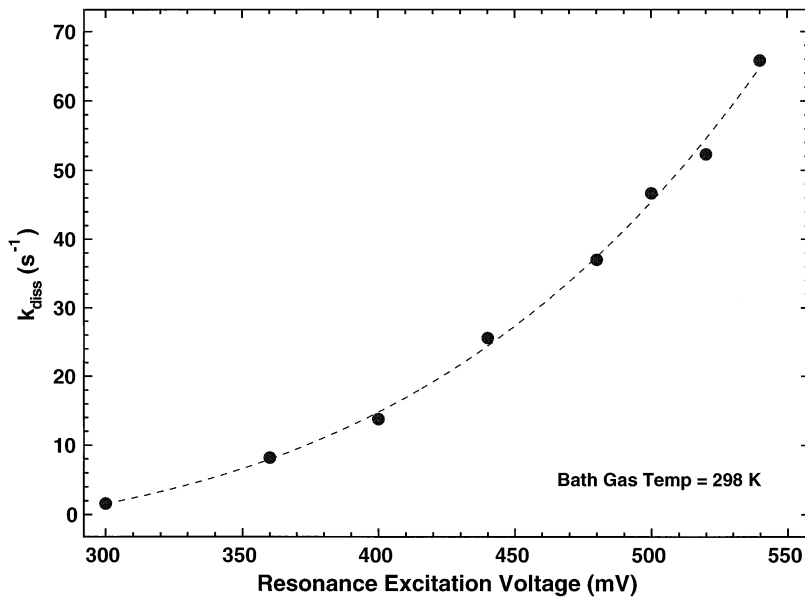
where  $A$  is the preexponential factor and  $E_a$  is the Arrhenius activation energy. By collecting  $k_{\text{diss}}$  data as a function of bath gas temperature over a  $k_{\text{diss}}$  range of 0.0273–0.244 s<sup>-1</sup> we have recently measured the Arrhenius parameters for protonated leucine enkephalin in the ion trap to be  $\log A = 12.55 \pm 0.87$  and  $E_a = 1.28 \pm 0.08$  eV [40]. Master equation modeling suggests that high pressure limit conditions apply over this  $k_{\text{diss}}$  range (see below). However, the direct use of the Arrhenius equation may be inappropriate for the conditions and dissociation rates applicable to this study (viz. 1.6–65 s<sup>-1</sup>). The Arrhenius equation assumes that high pressure limit (or rapid energy exchange) conditions apply and any error associated with its use is expected to increase with  $k_{\text{diss}}$ . That is, as  $k_{\text{diss}}$  increases the dissociation kinetics can move into the so-called roll-over region where the contribution from the activation rate becomes increasingly important relative to the contributions from the temperature (internal energy) dependent unimolecular dissociation rate constants [9,26].

The extent to which protonated leucine enkephalin ions undergoing ion trap collisional activation deviate from high pressure limit conditions can be estimated





(A)



(B)

Fig. 3. (a)  $\ln [MH^+]_t / [MH^+ + \Sigma P^+]_t$  vs. time plots for a series of resonance excitation voltages ( $q_z = 0.163$ , bath gas temperature = 298 K). (b) A plot of the  $k_{\text{diss}}$  obtained from the slopes of the data in Fig. 3(a) vs. monopolar resonance excitation voltage.

via master equation modeling of the activation, deactivation, and dissociation processes. We have described an approach to modeling collisional energy exchange in the ion trap [29] and have coupled this

with Rice–Ramsperger–Kassel–Marcus (RRKM) theory to account for unimolecular dissociation [30]. Using the critical energy and reactant ion and transition state vibrational frequencies employed by

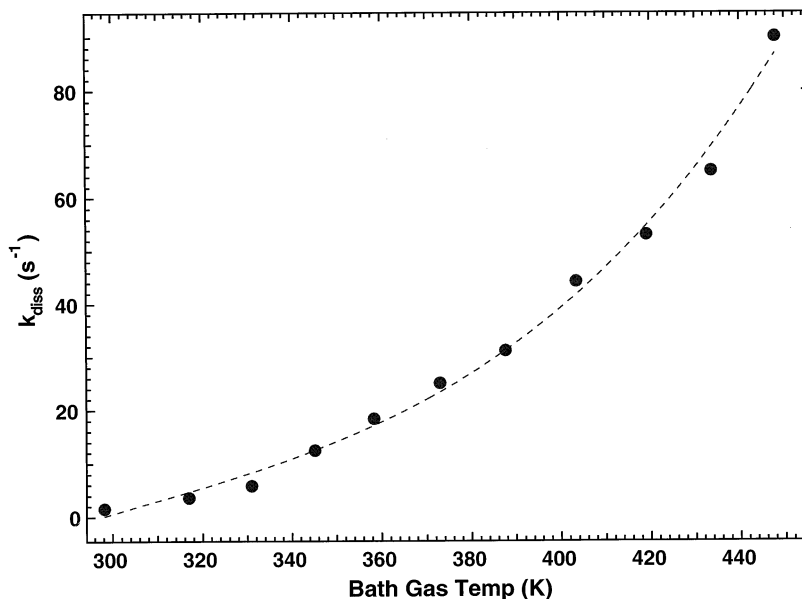


Fig. 4. A plot of  $k_{\text{diss}}$  vs. bath gas temperature using a fixed monopolar resonance excitation voltage of 300 mV.

Schnier et al. in their blackbody infrared dissociation study of protonated leucine enkephalin [41], we have used this approach to model the  $k_{\text{diss}}$  versus  $T_{\text{int}}$  behavior under the experimental conditions used in this study. A key parameter in modeling the rates of collisional energy transfer is the average internal energy down-step size,  $\alpha$ , associated with an ion/helium collision. By microscopic reversibility,  $\alpha$ , also determines the average size of an internal energy up-step. For this work, we used a relation for  $\alpha$  of

$$\alpha = 0.625kT + 0.001k(T_{\text{int}} - T) \quad (2)$$

where  $T$  is the bath gas temperature. This relationship gives an average energy step size of roughly  $130 \text{ cm}^{-1}$ , which is near the low end of the range of values reported for relatively small polyatomic ions in collisions with helium [52,53]. The use of a relatively small, average energy step size in the master equation modeling is expected to lead to conservative predictions of the activation and deactivation rates. We therefore expect that the master equation model, using a relatively small energy step size, more likely overestimates the magnitude of deviation from the high pressure limit behavior than underestimates it. Fig. 5 shows a plot indicating the value of  $\ln k_{\text{diss}}$  derived

from master equation modeling (dashed line) versus  $(kT_{\text{int}})^{-1}$  along with the expected high pressure limit behavior (solid line) as determined from the Arrhenius equation using the activation parameters cited above. Note that master equation modeling yields the expected high pressure limit result at  $T_{\text{int}}$  values of about 525 K and below. This corresponds to  $k_{\text{diss}}$  values of about  $1 \text{ s}^{-1}$  and below. Increasingly large deviations from high pressure limit behavior are predicted as  $T_{\text{int}}$  increases beyond about 525 K, indicating that ions fragmenting at rates significantly greater than roughly  $1 \text{ s}^{-1}$  are in the roll-over region. Almost all of the experimental values of  $k_{\text{diss}}$  reported here significantly exceed  $1 \text{ s}^{-1}$ .

As an ion population deviates further from high pressure limit behavior, the internal energy distribution deviates further from being a true Boltzmann distribution. Specifically, the ions in the high energy side of the distribution are depleted by fragmentation such that the distribution appears to be truncated at the high energy side. In this study, we are primarily concerned with the ion internal temperatures that can be achieved via ion trap collisional activation under normal conditions, rather than in the shape of the internal energy distribution of the ions that fragment



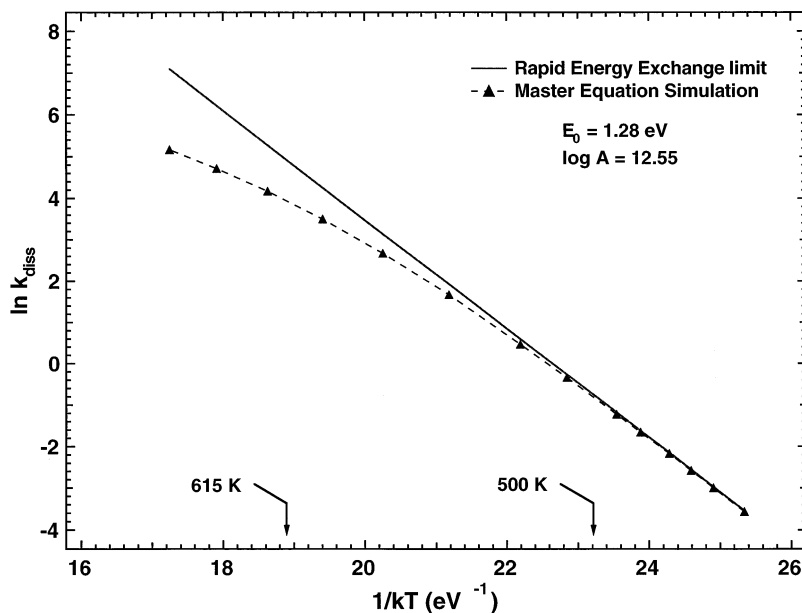


Fig. 5. Plot of the natural logarithm of the dissociation rate,  $\ln k_{\text{diss}}$ , as a function of  $(kT_{\text{int}})^{-1}$  as predicted by master equation modeling under high pressure limit conditions (solid line) and under the experimental conditions used in this study (dashed line).

at relatively high rates. The shape of such a truncated Boltzmann distribution is dependent upon the energetic and entropic requirements of the dissociation reaction(s) and is therefore expected to be somewhat ion specific. The relationship between  $T_{\text{int}}$  and resonance excitation voltage, as well as other factors that affect energy deposition, is of more general interest. It is possible to estimate the dependence of  $T_{\text{int}}$  on resonance excitation amplitude from the plot of Fig. 5 by use of the master equation model results (dashed line) as a calibration for the functional dependence of  $k_{\text{diss}}$  on  $T_{\text{int}}$ . Such a calibration is necessary because it appears that the Arrhenius equation cannot be used directly to relate  $k_{\text{diss}}$  to  $T_{\text{int}}$  over the dissociation rate range observed in this work. However, the accuracy of the master equation prediction depends upon several assumed parameters that include critical energy, vibrational frequencies of the reactant ion and transition state, and factors that determine the rates of activation and deactivation, such as  $\alpha$ .

A more attractive approach to determining the relationship between  $k_{\text{diss}}$  and  $T_{\text{int}}$  is to use the Arrhenius equation at low values of  $k_{\text{diss}}$ , where the

master equation prediction and the Arrhenius equation prediction agree, and to derive an empirical correlation at higher rates by varying the bath gas temperature. Fig. 6(a) shows a plot of  $T_{\text{int}}$ , calculated using the Arrhenius equation (dashed line), versus bath gas temperature obtained from  $k_{\text{diss}}$  values collected using a fixed resonance excitation amplitude of 300 mV (see Fig. 4 for  $k_{\text{diss}}$  versus bath gas temperature plot). In this case, a linear dependence with a slope of unity is expected, provided the parent ions are in the rapid energy exchange limit, because the contributions to  $T_{\text{int}}$  from ion acceleration and from the bath gas are additive [29].  $T_{\text{int}}$  as determined by direct application of the Arrhenius equation to the  $k_{\text{diss}}$  data clearly does not increase linearly with bath gas temperature, which is consistent with the master equation modeling prediction that high pressure limit behavior is not expected over this range of  $k_{\text{diss}}$  values. The solid line in Fig. 6(a) was constructed by calculating  $T_{\text{int}}$  at a bath gas temperature of 298 K and a resonance excitation amplitude of 300 mV using the Arrhenius equation ( $k_{\text{diss}} = 1.6 \text{ s}^{-1}$ ) and assuming a linear (slope of unity) increase in  $T_{\text{int}}$  with increasing bath gas tem-

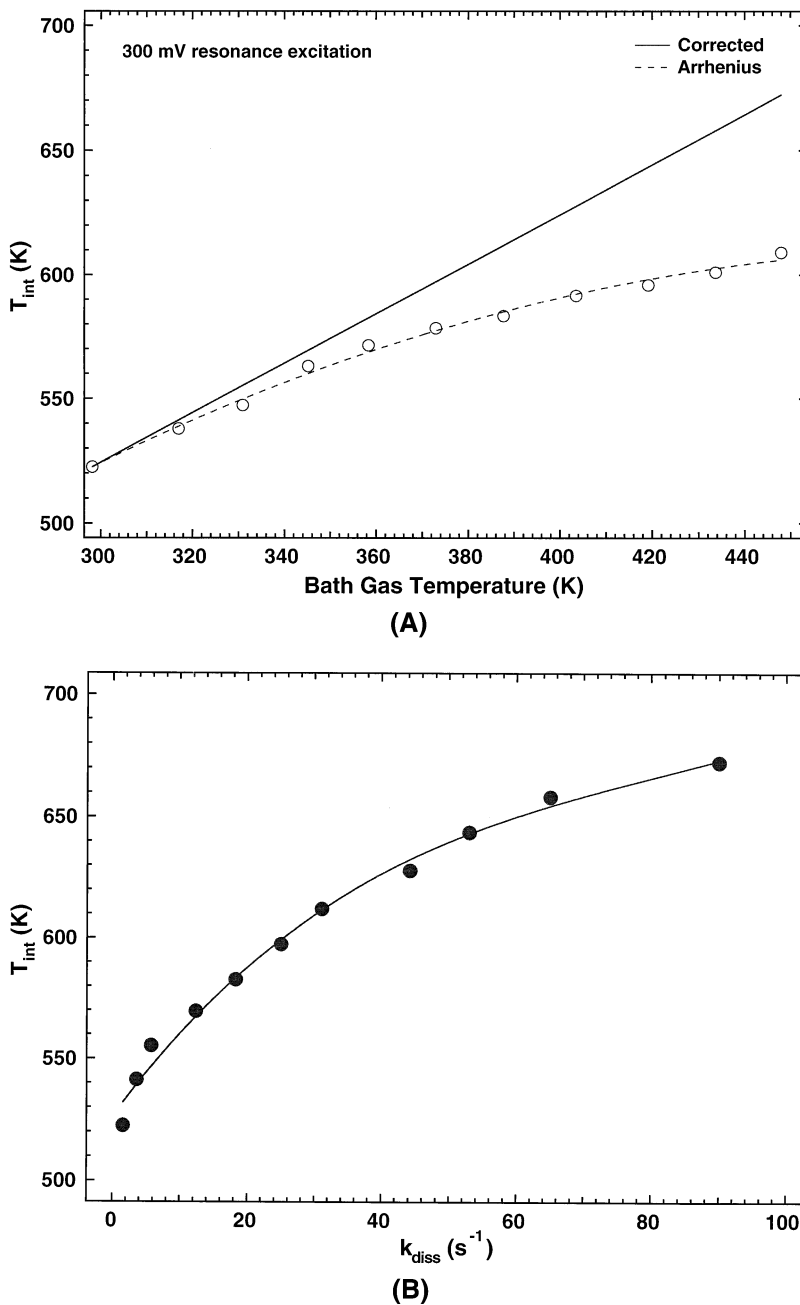


Fig. 6. (a) Plots of  $T_{\text{int}}$  vs. bath gas temperature using a resonance excitation amplitude of 300 mV (monopolar) obtained from experimental  $k_{\text{diss}}$  values using the Arrhenius equation (open circles, dashed line) and a theoretical prediction based on use of the Arrhenius equation to establish  $T_{\text{int}}$  at  $k_{\text{diss}} = 1.6 \text{ s}^{-1}$  (300 mV, 298 K) and assuming a linear relationship between  $T_{\text{int}}$  and the temperature of the bath gas (solid line). (b) The relationship between  $T_{\text{int}}$  and  $k_{\text{diss}}$  derived from plotting  $k_{\text{diss}}$  values obtained as a function of bath gas temperature (monopolar resonance excitation = 300 mV) against the corresponding temperatures on the solid line of (a).

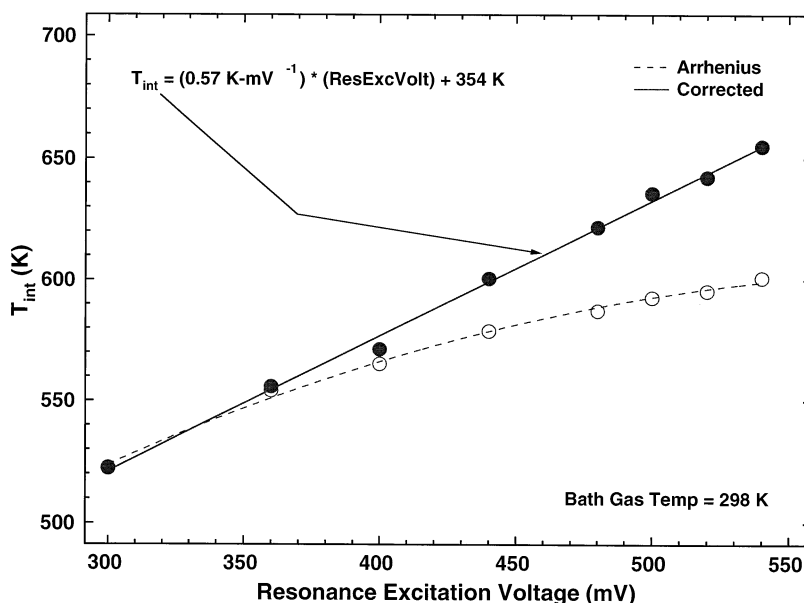


Fig. 7. Plots of  $T_{int}$  vs.  $V$ , where  $T_{int}$  was determined directly from the Arrhenius equation (open circles, dashed line) and from the  $T_{int}$  vs.  $k_{diss}$  calibration of Fig. 6(b) (filled circles, solid line). Error bars associated with the  $k_{diss}$  measurements fall within the areas of the filled and open circles.

perature. This plot represents a prediction of the parent ion internal temperature provided the ions show high pressure limit behavior over the entire range of  $k_{diss}$ . (Alternatively, the solid line plot predicts the  $T_{int}$  versus bath gas temperature behavior at a resonance excitation voltage of 300 mV for an ion population that does not fragment. A nonfragmenting ion population has a Boltzmann distribution of internal energies because the high energy side is not depleted by fragmentation.) The solid line of Fig. 6(a) can therefore be used to relate  $k_{diss}$  to  $T_{int}$ . The resulting relationship between  $T_{int}$  and  $k_{diss}$  derived from plotting  $k_{diss}$  values obtained as a function of bath gas temperature (resonance excitation = 300 mV) versus the corresponding temperatures on the solid line of Fig. 6(a) is shown in Fig. 6(b). Fig. 6(b) can be used to relate  $k_{diss}$  to  $T_{int}$  for protonated leucine enkephalin using any continuous form of ion activation including, among others, thermal dissociation, resonance excitation (monopolar, dipolar, or quadrupolar [44]), and continuous wave infrared multiphoton dissociation [54–56].

Fig. 7 shows plots of  $T_{int}$  versus  $V$  where  $T_{int}$  is

derived directly from the Arrhenius equation (open circles, dashed line) using the  $k_{diss}$  values from Fig. 3(b) and the Arrhenius parameters listed above, and using the calibration of  $T_{int}$  versus  $k_{diss}$  obtained from Fig. 6(b) (filled circles, solid line). It is clear that the  $T_{int}$  values calculated from the Arrhenius equation increase with resonance excitation amplitude, as expected, but that the dependence is somewhat less than linear. This behavior is expected because both the master equation model and the bath gas temperature experiments leading to Fig. 6 suggest that the protonated leucine enkephalin ions are in the roll-over region over at least most of this  $k_{diss}$  range. The solid line (filled circles) results account for this effect and indicate that there is a linear relationship (correlation coefficient,  $r = 0.9985$ ) between  $T_{int}$  and resonance excitation voltage, at least over the range of 300–540 mV. The sensitivity of  $T_{int}$  to resonance excitation voltage (slope of the line) is about  $0.57 \text{ K}\cdot\text{mV}^{-1}$  and the total temperature increase effected over the range of resonance excitation amplitudes used here (300–540 mV) is about 133 K. Furthermore, the data suggest that the parent ions are elevated by about 357

K over the bath gas temperature (655 – 298 K) at a resonance excitation voltage of 540 mV. The y intercept of the solid line is about 354 K; this is higher than the expected bath gas temperature value [40]. However, the experimental error associated with the y intercept is relatively large (about  $\pm 50$  K). When an additional data point of 298 K at 0 mV is used to plot  $T_{\text{int}}$  versus  $V$  (plot not shown), a straight line ( $r^2 = 0.996$ ) of slope  $0.656 \text{ K}\cdot\text{mV}^{-1}$  and intercept of 308 K is obtained. These results suggest that the relationship between  $T_{\text{int}}$  and (frequency optimized) resonance excitation voltage is very nearly linear over a wide range of values. A slight decrease in slope at increasing voltages cannot be precluded from these data, however. It must also be recognized that these data were collected under conditions in which resonance ejection of the parent ions, a process that eventually becomes dominant at high resonance excitation voltages, was minimal. Hence, these data reflect the dependence of  $T_{\text{int}}$  on resonance excitation amplitude in which losses of parent ions due to ejection make little or no contribution.

A linear relationship between steady-state ion oscillatory amplitude and  $V$  is expected with a pure quadrupolar field under conditions in which ion acceleration and deceleration (due to ion/bath gas collisions) are equal. A linear relationship between  $T_{\text{int}}$  and  $V$  over this range of  $V$  would therefore be expected under such conditions as well [29]. These studies were conducted using an ion trap with higher order fields intentionally imposed, thereby introducing some nonlinear character to ion acceleration as a function of resonance excitation voltage [32,57]. This effect might be expected to lead to a greater than linear increase in  $T_{\text{int}}$  with  $V$ . On the other hand, the change in ion frequency with oscillatory amplitude that results from the presence of higher order fields implies that ions may not always be in optimal resonance with the excitation voltage. The potential for ions falling out of resonance with the applied signal increases with excitation voltage. The possible detuning effect whereby ion oscillation can increase and then decrease due to dephasing, in analogy with the technique of sustained off-resonance irradiation used for collisional activation in an ion cyclotron

resonance spectrometer [58], might lead to a less than linear increase in  $T_{\text{int}}$  with excitation voltage. The studies reported here suggest that, at least under the conditions thus far explored, collisional activation in commonly employed ion traps shows a roughly linear dependence of  $T_{\text{int}}$  upon  $V$ , provided the resonance excitation frequency is tuned to give the maximum  $k_{\text{diss}}$ .

#### 4. Conclusions

These studies suggest that there is a linear relationship between the internal temperature to which a high-mass ion can be elevated under single-frequency resonance excitation conditions and the amplitude of the frequency-optimized voltage. Such a relationship is expected for a pure quadrupolar field and also appears to be observed with a commonly used ion trap geometry in which higher order fields have been intentionally imposed. The internal temperature of a parent ion undergoing collisional activation can be increased in two general ways. The most common means is to accelerate the ion by use of resonance excitation. Another means is to increase the kinetic energy of the bath gas (i.e. raise its temperature). By systematically varying the bath gas temperature it is possible to determine the relationship between the change in dissociation rate of an ion as a function of the change in its internal temperature. This information is then useful in determining the relationship between ion internal temperature and parameters that affect ion acceleration, such as the resonance excitation voltage. Whereas elevating the bath gas temperature as a means for collisional activation has important uses, ion acceleration via externally imposed electric fields is far more convenient and allows for a measure of control of ion internal energy during the course of an ion trap experiment that is lacking with static bath gas temperature experiments. Furthermore, these studies indicate that the internal temperature of an ion of mass 556 Da can be elevated by about 357 K over the temperature of the bath gas (to 655 K in this case). This value was derived from a dissociation rate of  $65.8 \text{ s}^{-1}$ . Dissociation rates for protonated

leucine enkephalin in the ion trap several times higher than this have been observed. The value of 655 K, therefore, does not constitute an upper limit to the internal temperature to which an ion of mass 556 Da can be elevated by collisional activation in an ion trap. These studies were conducted under conditions in which ion ejection, the process that ultimately limits the internal temperature to which ions can be raised above the bath gas temperature using an ion acceleration technique, was minimal.

### Acknowledgements

This research was sponsored by the Division of Chemical Sciences, Office of Basic Energy Sciences, U.S. Department of Energy, under Contract DE-AC05-96OR22464 with Oak Ridge National Laboratory, managed by Lockheed Martin Energy Research Corp. Professor Evan Williams and Dr. Paul Schnier of the University of California at Berkeley are gratefully acknowledged for providing the vibrational frequencies they used to model the leucine enkephalin ions in their blackbody infrared radiative dissociation study of these ions. Dr. James L. Stephenson Jr. is acknowledged for his valuable assistance and advice throughout the course of this study. Dr. Gary J. Van Berkel is acknowledged for construction of the electrospray source used in this study.

### References

- [1] F.W. McLafferty (Ed.), *Tandem Mass Spectrometry*, Wiley, New York, 1983.
- [2] K.L. Busch, G.L. Glish, S.A. McLuckey, *Mass Spectrometry/Mass Spectrometry: Techniques and Applications of Tandem Mass Spectrometry*, VCH, New York, 1988.
- [3] K. Vékey, *J. Mass Spectrom.* 31 (1996) 445.
- [4] M.S. Kim, F.W. McLafferty, *J. Am. Chem. Soc.* 100 (1978) 3279.
- [5] S.H. Lee, M.S. Kim, J.H. Beynon, *Int. J. Mass Spectrom. Ion Processes* 75 (1987) 83.
- [6] K. Vékey, A.G. Brenton, J.H. Beynon, *J. Phys. Chem.* 90 (1986) 3569.
- [7] H.I. Kenttämä, R.G. Cooks, *Int. J. Mass Spectrom. Ion Processes* 64 (1985) 79.
- [8] V.H. Wysocki, H.I. Kenttämä, R.G. Cooks, *Int. J. Mass Spectrom. Ion Processes* 75 (1987) 181.
- [9] S.A. McLuckey, D.E. Goeringer, *J. Mass Spectrom.* 32 (1997) 461.
- [10] L.R. Thorne, J.L. Beauchamp, in M.T. Bowers (Ed.), *Gas Phase Ion Chemistry*, Academic, New York, 1984, Volume 3, Chap. 18.
- [11] R.C. Dunbar, in M.T. Bowers (Ed.), *Gas Phase Ion Chemistry*, Academic, New York, 1979, Vol. 2, Chap. 14.
- [12] R.C. Dunbar, in M.T. Bowers (Ed.), *Gas Phase Ion Chemistry*, Academic, New York, 1984, Vol. 3, Chap. 20.
- [13] R.C. Dunbar, *J. Chem. Phys.* 95 (1991) 2537.
- [14] R.C. Dunbar, R.C. Zaniewski, *J. Chem. Phys.* 96 (1992) 5069.
- [15] G.T. Uechi, R.C. Dunbar, *J. Chem. Phys.* 96 (1992) 8897.
- [16] G.T. Uechi, R.C. Dunbar, *J. Chem. Phys.* 98 (1993) 7888.
- [17] R.C. Dunbar, T.B. McMahon, *Science* 279 (1998) 194.
- [18] D. Thölmann, D.S. Tonner, T.B. McMahon, *J. Phys. Chem.* 98 (1994) 2002.
- [19] D.S. Tonner, D. Thölmann, T.B. McMahon, *Chem. Phys. Lett.* 233 (1995) 324.
- [20] R.C. Dunbar, *J. Phys. Chem.* 98 (1994) 8705.
- [21] R.C. Dunbar, T.B. McMahon, D. Thölmann, D.S. Tonner, D.R. Salahub, D. Wei, *J. Am. Chem. Soc.* 117 (1995) 12 819.
- [22] C.Y. Lin, R.C. Dunbar, *J. Phys. Chem.* 100 (1996) 655.
- [23] W.D. Price, P.D. Schnier, E.R. Williams, *Anal. Chem.* 68 (1996) 859.
- [24] P.D. Schnier, W.D. Price, R.A. Jockusch, E.R. Williams, *J. Am. Chem. Soc.* 118 (1996) 7178.
- [25] W.D. Price, P.D. Schnier, R.A. Jockusch, E.F. Strittmatter, E.R. Williams, *J. Am. Chem. Soc.* 118 (1996) 10 640.
- [26] W.D. Price, E.R. Williams, *J. Phys. Chem.* 101 (1997) 8844.
- [27] J.N. Louris, R.G. Cooks, J.E.P. Syka, P.E. Kelley, G.C. Stafford Jr., J.F.J. Todd, *Anal. Chem.* 59 (1987) 1677.
- [28] J.V. Johnson, C. Basic, R.E. Pedder, B.L. Kleintop, R.A. Yost, in *Practical Aspects of Ion Trap Mass Spectrometry*, R.E. March, J.F.J. Todd (Eds.), CRC, Boca Raton, 1995, Volume III, p. 267.
- [29] D.E. Goeringer, S.A. McLuckey, *J. Chem. Phys.* 104 (1996) 2214.
- [30] D.E. Goeringer, S.A. McLuckey, *Rapid Commun. Mass Spectrom.* 10 (1996) 328.
- [31] J.E.P. Syka, in *Practical Aspects of Ion Trap Mass Spectrometry*, R.E. March, J.F.J. Todd (Eds.), CRC, Boca Raton, 1995, Volume I, p. 169.
- [32] J. Franzen, R.-H. Gabling, M. Schubert, Y. Wang, in *Practical Aspects of Ion Trap Mass Spectrometry*, R.E. March, J.F.J. Todd (Eds.), CRC, Boca Raton, 1995, Volume 1, p. 49.
- [33] C. Paradisi, J.F.J. Todd, P. Traldi, U. Vettori, *Org. Mass Spectrom.* 27 (1992) 1210.
- [34] P. Liere, T. Blasco, R.E. March, J.C. Tabet, *Rapid Commun. Mass Spectrom.* 8 (1994) 953.
- [35] J.B. Plomely, F.A. Londry, R.E. March, *Rapid Commun. Mass Spectrom.* 10 (1996) 200.
- [36] P. Liere, R.E. March, T. Blasco, J.C. Tabet, *Int. J. Mass Spectrom. Ion Processes* 153 (1996) 101.
- [37] D.E. Goeringer, S.A. McLuckey, *Int. J. Mass Spectrom.* (unpublished).

- [38] K.J. Hart, S.A. McLuckey, *J. Am. Soc. Mass Spectrom.* 5 (1994) 250.
- [39] A. Colorado, J. Brodbelt, *J. Am. Soc. Mass Spectrom.* 7 (1996) 1116.
- [40] K.G. Asano, D.E. Goeringer, S.A. McLuckey, *Int. J. Mass Spectrom.* (unpublished).
- [41] P.D. Schnier, W.D. Price, E.F. Strittmatter, E.R. Williams, *J. Am. Soc. Mass Spectrom.* 8 (1997) 771.
- [42] M. Meot-Ner, A.R. Dongré, Á. Somogyi, V.H. Wysocki, *Rapid Commun. Mass Spectrom.* 9 (1995) 829.
- [43] G.J. Van Berkel, G.L. Glish, S.A. McLuckey, *Anal. Chem.* 62 (1990) 1284.
- [44] R.E. March, A.W. McMahon, F.A. Londry, R.L. Alfred, J.F.J. Todd, F. Vedel, *Int. J. Mass Spectrom. Ion Processes* 95 (1989) 119.
- [45] C. Paradisi, J.F.J. Todd, P. Traldi, U. Vettori, *Rapid Commun. Mass Spectrom.* 6 (1992) 641.
- [46] R.E. March, M.S. Weir, M. Tkaczyk, F.A. Londry, R.L. Alfred, A.M. Franklin, J.F.J. Todd, *Org. Mass Spectrom.* 28 (1993) 499.
- [47] C. Paradisi, P. Traldi, U. Vettori, *Rapid Commun. Mass Spectrom.* 7 (1993) 690.
- [48] A.D. Penman, J.F.J. Todd, D.A. Thorner, R.D. Smith, *Rapid Commun. Mass Spectrom.* 4 (1990) 415.
- [49] J.V. Johnson, R.E. Pedder, R.A. Yost, *Rapid Commun. Mass Spectrom.* (1992) 247.
- [50] J.D. Williams, K.A. Cox, R.G. Cooks, S.A. McLuckey, K.J. Hart, D.E. Goeringer, *Anal. Chem.* 66 (1994) 725.
- [51] M.J. Charles, S.A. McLuckey, G.L. Glish, *J. Am. Soc. Mass Spectrom.* 5 (1994) 1031.
- [52] R.G. Gilbert, *J. Chem. Phys.* 80 (1984) 5501.
- [53] A.T. Barfknecht, J.I. Brauman, *J. Chem. Phys.* 84 (1986) 3870.
- [54] R.J. Hughes, R.E. March, A.B. Young, *Int. J. Mass Spectrom. Ion Phys.* 42 (1982) 255.
- [55] J.L. Stephenson Jr., M.M. Booth, J.A. Shalosky, J.R. Eyler, R.A. Yost, *J. Am. Soc. Mass Spectrom.* 5 (1994) 886.
- [56] A. Colorado, J.X. Shen, V.H. Vartanian, J. Brodbelt, *Anal. Chem.* 68 (1996) 4033.
- [57] M. Splendore, F.A. Londry, R.E. March, R.J.S. Morrison, P. Perrier, J. André, *Int. J. Mass Spectrom. Ion Processes* 156 (1996) 11.
- [58] J.W. Gauthier, T.R. Trautman, D.B. Jacobson, *Anal. Chim. Acta* 246 (1991) 211.